Published in final edited form as:
Heart Rhythm. 2007 November ; 4(11): 1430–1436.

Optical Measurements of Intramural Action Potentials in Isolated Porcine Hearts Using Optrodes

Wei Kong, PhD, **Nadia Fakhari, MS**, **Oleg F. Sharifov, MD, PhD**, **Raymond E. Ideker, MD, PhD**, **William M. Smith, PhD**, and **Vladimir G. Fast, PhD**

Abstract

Background—Measurements of intramural V_m would greatly increase knowledge of cardiac arrhythmias and defibrillation. Optrodes offer the possibility for three-dimensional V_m mapping but their signal quality has been inadequate.

Objectives— The objectives of this work were to improve optrode signal quality and use optrodes to measure intramural distribution of action potentials and shock-induced V_m changes in porcine hearts.

Methods—Optrodes were made from seven optical fibers 225 or 325 μm in diameter. Fiber ends were polished at 45° angle which improved light collection and allowed their insertion without a needle. Fluorescent measurements were performed in isolated porcine hearts perfused with Tyrode's solution or blood using V_m-sensitive dye RH-237 and a 200-W Hg/Xe lamp.

Results—The signal-to-noise ratio for 325-μm fibers was 44±23 in blood-perfused hearts (n=5) and 106±45 in Tyrode-perfused hearts (n=3), which represents a ≈4-fold improvement over previously reported data. There was close correspondence between optical and electrical measurements of activation times and action potential duration (APD). No significant intramural APD gradients were observed at cycle lengths up to 4 s and in the presence of dofetilide or d-sotalol. Application of shocks (5–50 V/cm) produced large intramural V_m changes (up to ≈200%APA) possibly reflecting a combined effect of tissue discontinuities and optrode geometry.

Conclusions—A substantial improvement of optrode signal quality was achieved. Optical measurements of APD and activation times matched electrical measurements. Optrode measurements revealed no significant intramural APD gradients. Application of shocks caused large intramural V_m changes that could be influenced by the optrode geometry.

Keywords

cardiac excitation; action potentials; defibrillation; virtual electrodes; optical mapping; fiber optics

Introduction

Optical mapping of electrical activation has become an important research tool in cardiac electrophysiology.[1] This method employs fluorescent dyes and arrays of photodetectors to measure changes in membrane potential (V_m) at multiple locations on the heart surface. Optical mapping offers several advantages over electrical mapping techniques including the ability to

Address for correspondence: Vladimir G. Fast, PhD, Department of Biomedical Engineering, University of Alabama at Birmingham, 1670 University Blvd., VH B126, Birmingham, AL, 35294, Phone: (205) 975-2119, Fax: (205) 975-4720, E-mail: fast@crml.uab.edu.

measure the repolarization phase of the action potential as well as V_m changes caused by electrical shocks. In addition, optical mapping allows for simultaneous measurements of V_m and other electrophysiological parameters such as intracellular calcium concentration.[2–5] Optical mapping has been employed in various experimental preparations ranging from single cells to whole hearts to study mechanisms of impulse propagation,[6,7] cardiac arrhythmias[8–14] and defibrillation.[15,16]

Although application of optical mapping in cardiac electrophysiology has been very successful, it has important limitations. Unlike electrical mapping, which allows measurements both from the heart surface and from intramural muscle layers,[17–19] optical mapping was until recently restricted to the heart surface. However, information on the three-dimensional V_m dynamics is critically important for understanding the mechanisms of cardiac arrhythmias and defibrillation. Thus, electrical mapping studies using plunge needle electrodes demonstrated that the source of ventricular fibrillation may be intramural.[20] Microelectrode recordings and optical mapping in wedge preparations revealed large transmural heterogeneities of action potential duration (APD) that may play an important role in arrhythmogenesis.[21,22] Intramural shock-induced V_m changes are believed to be critical for defibrillation.[16,23] Investigation of these phenomena requires three-dimensional mapping of V_m in intact hearts but no such methods are currently available.

To circumvent this limitation, a new optical technique was introduced recently,[24,25] which employs fiber-optic technology. In this method, bundles of optical fibers (“optrodes”) are used to deliver excitation light to intramural tissue layers and to collect the emitted fluorescence, which is measured with arrays of photodiodes. The initial optrode studies demonstrated the feasibility of this approach for V_m measurements at multiple sites across left ventricular wall. These studies also exposed several limitations of optrode recordings that hinder the extension of this technology to fully three-dimensional mapping. One important limitation of current optrodes is a relatively low signal-to-noise ratio, which is significantly smaller than in surface optical mapping. Such low signal quality precludes intramural optical measurements in hearts perfused by blood, which is preferable in long-lasting experiments on isolated hearts.[9] Therefore, the main goal of this work was to enhance the quality of optrode recordings by improving the optrode design and optimizing the optical system. The other goals were to use the new optrodes to characterize intramural distribution of action potentials in the left ventricle of porcine hearts, to compare optical recordings with electrical measurements and to measure intramural V_m changes caused by electrical shocks.

Methods

Optical Setup

The optical setup for intramural optrode recordings, schematically shown Figure 1A, was similar in its overall design to the one described previously[25] with several modifications. A stronger 200-W Hg/Xe lamp was used as an excitation light source which resulted in increased fluorescence. The excitation light was filtered at 530–585 nm, deflected by a dichroic mirror (>600 nm) and focused on optrode entrance by an objective lens (5x Fluar, Carl Zeiss Inc.). The emitted fluorescence was collected by the same lens, passed through the dichroic mirror and filtered at >650 nm. The fluorescent light was converted to voltages using a 16×16 photodiode array (PDA) integrated with current-to-voltage converters with 100-MΩ feedback resistors (model C4675–102, Hamamatasu Corp.). Electrical signals were conditioned using a 256-channel set of 2nd-stage amplifiers (Innovative Technologies) and digitized at a 12-bit resolution and a sampling interval of 0.512 ms using a data acquisition system which consisted of four 64-channel data acquisition cards (PCI-6071E, National Instruments) installed in a PC. An additional 8-channel digital card (PCI-6602, National Instruments) was used to control stimulation, light excitation, shock application, and change of amplifier parameters.

Optrodes

Optrodes were made from silicon fibers with an outer diameter of 225 or 325 μm (FT-200-URT and FT-300-UMT, Thorlabs Incs.). These fibers have core diameters of 200 and 300 μm, respectively, and numerical apertures of 0.50 and 0.39, respectively. Each optrode consisted of 9 fibers. Seven fibers were used to record optical signals and two other fibers were used for optrode-PDA alignment. At one end (tissue end), seven fibers were polished at approximately 45° to the fiber axis. This was different from the previous work[25] where flat-cleaved fibers were used. Polishing fibers resulted in a closer contact with the tissue and better light collection. In addition, optrodes made from polished fibers could be introduced into the heart without the aid of an insertion needle, which reduced the extent of tissue damage. This made possible the use of the larger 325-μm fibers, which resulted in much higher signal levels with less tissue damage in comparison to the previous study.[25] Fibers were arranged in a hexagonal pattern as shown in Figure 1B with fiber ends spaced 2 or 3 mm apart. At the other end (detector end), fibers were polished perpendicular to the fiber axis and arranged in a line (Figure 1C). Two additional alignment fibers were prepared in the same fashion but with both ends polished perpendicular to the fiber axis and placed on both sides of the linear fiber array.

The optrode detector end and the PDA were mounted on micro-positioners. Their mutual alignment was performed by shining light from a light-emitting diode (LED) at the alignment fibers and measuring optical signals at corresponding diodes of the PDA. The optrode-lens and the lens-PDA distances as well as lateral positions of all optical elements were adjusted until the maximal cross-talk between the diodes receiving light from the alignment fibers and any other diode in their immediate vicinity became less than 3%.

The quality of fiber preparation was examined by immersing an optrode into a 6-μmol/L solution of rhodamine and measuring its fluorescence. The fibers were considered acceptable if the differences in signal magnitudes between all seven fibers were less than 30% of the maximum signal magnitude.

Porcine heart preparation

The investigation conformed to the Guide for the Care and Use of Laboratory Animals published by the US National Institutes of Health (NIH Publication No. 85–23, revised 1996). Pigs with a weight of ≈25 kg of either sex were anesthetized with Telazol (4.4 mg/Kg), Xylazine (4.4 mg/Kg) and Antropine (0.04 mg/Kg). Anesthesia was maintained with inhalation of Isoflurane (1.3–2.5%) in oxygen. If blood was used for heart perfusion, a warm Tyrode's solution(in mmol/l, NaCl 128.5, Glucose 20, KCl 4.7, $MgCl_2$ 0.7, NaH_2PO_4 0.5, $CaCl_2$ 1.5, and $NaHCO_3$ 28) was infused in the carotid vein and the blood was drained from the carotid artery. Heart contraction was stopped by KCl injection or by the application of a 9 V battery to induced fibrillation. The heart was quickly removed from the chest and placed in a cold physiological solution. After weighing the heart, the aorta was cannulated and the heart was retrogradely perfused with either Tyrode's solution or blood. The perfusate temperature was maintained at 37°C and was bubbled with a mixture of 95% O_2 and 5% CO_2. The flow rate was maintained at approximately 1 mL/min per 1 g of heart weight. At the end of the experiments, the heart was weighted again to estimate the degree of tissue edema. The LV wall was dissected to determine the wall thickness.

To enable external pacing, the sinus node was removed. Hearts were paced using a bipolar electrode and a custom made stimulus generator at a cycle length (CL) of 0.5 s. Rectangular shocks with duration of 10 ms were applied via two large mesh electrodes sutured to the LV and RV epicardium using a custom-made current pulse generator. An optrode was inserted through a whole at the center of the mesh LV electrode. Intramural shock strength was

measured using a bipolar plunge needle electrode inserted approximately 5 mm away from the optrode.

For optical measurements, hearts were stained with fluorescent V_m-sensitive dye RH-237. The dye was diluted in 10 mL of Tyrode's solution at a concentration of 0.25 mmol/L. This solution was injected into a perfusion line at a rate of 3.3 ml/min for 3 min using a syringe pump. The estimated dye concentration in the perfusion solution during injection was 5.5 μmol/L. To prevent motion artifacts in optical recordings, excitation-contraction uncoupler 2,3-butanedione monoxime was added to the perfusion solution at a concentration of 15–25 mmol/L.

Optrode recordings

An optrode was inserted into the free anterior LV wall perpendicular to the epicardium. Recording sites were at a depth of 2 to 14 mm (2-mm optrode) or 3 to 21 mm (3-mm optrode). If necessary, optical signals were low-pass filtered to reduce noise. AP amplitude (APA) was determined as a difference in optical levels measured before and after an upstroke. Activation times (AT_o) were measured at a moment of 50% of AP upstroke. The signal-to-noise ratio (SN_{rms}) was calculated from unfiltered signals as the ratio of APA and root-mean-square noise measured over a 20-ms time interval preceding the AP upstroke.

The APD was measured as a time interval between the AT and 80% level of repolarization (APD_{80}). Transmural APD gradients were measured in control conditions, at various CLs (0.5–4 s) and in the presence of potassium channel blockers d-sotalol (125 μmol/L) or dofetilide (2 μmol/L) that are known to augment intramural APD heterogeneity.[26,27] Optical recordings were compared with extracellular electrical recordings from a plunge needle electrode inserted near an optrode. Electrical activation times (AT_e) were measured at the moment of minimum derivative of the QRS complex. Activation-recovery intervals (ARI) were measured as the time difference between AT_e and the time of maximum derivative of the T wave.[28] The correlations between AT_o and AT_e as well as between APD_{80} and ARI were calculated using linear regression. Shock-induced V_m changes were measured as previously described.[16]

Results

Optrode signal quality

Figure 2 shows intramural action potentials recorded using 325-μm fiber optrodes in porcine hearts perfused either by Tyrode's solution (Panel A) or blood (Panel B). Measurements in Tyrode-perfused hearts had substantially higher SN_{rms} than the ones obtained in blood-perfused hearts. Recordings shown in Panels A and B had SN_{rms} of 154±86 and 58±16, respectively. Average SN_{rms} values obtained from all hearts were 106±46 for Tyrode perfusion (n=6 sites in 3 hearts) vs. 44±23 for blood perfusion (n=12 sites in 5 hearts, $p<0.001$). The highest SN_{rms} in Tyrode-perfused hearts could reach ≈300. When optrodes with narrower 225-μm fibers were used in Tyrode-perfused hearts (recordings not shown), SN_{rms} was 40±8 (n=7 sites in 6 hearts).

Signal quality decreased over time, likely due to dye washout and photobleaching. Panel C illustrates changes in SN_{rms} measured in a Tyrode-perfused heart. It shows that signal quality decreased by approximately 40% during a 1-hour time period. In 4 hearts, the average decrease of SN_{rms} over 1 hour was 33±7%.

Action potentials sometimes exhibited a triangular shape, which is exemplified by intramural AP at site 5 in Panel A. Such AP shape indicates local tissue ischemia.[29] Such AP shapes were observed more often in Tyrode-perfused hearts than in blood-perfused hearts. This could be partially attributed to tissue edema developed during the course of experiment, which was more

pronounced in Tyrode perfused hearts than in blood-perfused hearts. Over the duration of an experiment (≈4 hours), the heart weight increased by 118±34% in Tyrode-perfused hearts (n=3) and by 35±15% in blood-perfused hearts (n=3).

Comparison of optical and electrical recordings

Extracellular electrical recordings of ARI have been used as an estimate of intramural APD measurements,[28] which is based on the assumption that electrical AT and ARI match AT and APD obtained from V_m measurements. To validate this assumption, we compared optrode measurements of intramural V_m with electrical measurements from a nearby location.

Figure 3A shows examples of simultaneous optical and electrical recordings at different pacing CLs. ATs measured optically and electrically were very similar when CL was changed between 200 and 1000 ms. The average difference between AT_o and AT_e measured at all CLs was 1.3 ±1.4 ms. Similarly, repolarization times changed in parallel, which was reflected in a high correlation between optical APD_{80} and electrical ARI (R^2=0.98) upon changes of CL (Panel B).

Intramural APD heterogeneity

Intramural heterogeneity of APD, previously reported in studies on single cells and isolated wedge preparations, is considered an important factor in arrhythmogenesis. To examine the presence of APD gradients in porcine hearts, we measured intramural APD in the LV wall at various CLs and in the presence of drugs. The APD values obtained from different tissue depths were combined in three groups: sub-epicardial group (Sub-Epi) with APD measurements obtained at a depth of 2–4 mm; mid-myocardial group (Mid) with data obtained at a depth of 6–10 mm, and sub-endocardial group (Sub-Endo) with measurements from a depth of 12–14 mm.

In control conditions and pacing CL of 500 ms, no significant APD gradients were detected (Figure 4A). The average APD_{80} was 200±17, 199±18 and 205±28 ms in Sub-Epi, Mid, and Sub-Endo regions, respectively. The differences between all regions were not statistically significant. Increasing CL up to 4000 ms resulted in prolongation of average APD_{80} to 229 ±29 ($p<0.05$, comparison with APD_{80} at 500-ms CL), 225±25 ($p<0.05$) and 230±36 ms ($p<0.05$) in corresponding regions without increase in regional APD_{80} differences. Such degree of CL-dependent prolongation of APD is similar to previously reported data obtained from porcine heart preparations.[30]

Application of d-sotalol (Figure 4B) or dofetilide (Panel C) caused a statistically significant increase of APD_{80} ($p<0.05$ for both drugs) at all intramural regions but didn't increase intramural APD_{80} heterogeneities even at slow pacing rates. The increase of APD under the influence of these drugs is consistent with previous publications. [26,27]

Shock-induced ΔV_m

Figure 5A shows examples of intramural V_m changes caused by 10-ms shocks with strength of 8 V/cm applied during the AP plateau phase in one heart. Shocks produced significant polarizations at the majority of intramural locations. The ΔV_m magnitude was highly variable ranging between approximately 5%APA and 100%APA at different locations. In most cases, the sign of ΔV_m was reversed with changing the shock polarity.

Qualitatively similar findings were obtained in other cases. Panel B depicts maximal and minimal ΔV_m measured at different shock strengths in 5 preparations. Similarly to previous ΔV_m measurements in wedge preparations,[16] shock-induced polarizations were asymmetric with negative ΔV_m exceeding positive ΔV_m approximately 2-fold. Increasing shock strength

resulted in increase of both maximal and minimal ΔV_m that reached magnitudes of approximately 100%APA and 200%APA, respectively.

Discussion

Fiber optics technology allows for multi-site intramural V_m measurements in the heart. Extension of this technology to full 3-dimensional mapping depends on improvements in existing optrode techniques with regard to signal quality, reliability and ease of use. The present work achieved a significant improvement in the quality of optrode recordings using a standard optical design. These optrodes were tested by measurements of intramural APD, comparison of optical and electrical recordings and shock-induced ΔV_m in porcine hearts.

Optrode signal quality

One of the most important parameters of optical recordings is the SN_{rms}. In comparison to our previous study,[25] which employed the same overall optical system design, the SN_{rms} value was approximately doubled when using optrodes made from 225-μm fibers and increased 4-fold when using the 325-μm fibers. The gain in SN_{rms} was due to several factors. One of them was the use of a brighter 200-W Hg/Xe lamp instead of a 100-W Hg lamp. Another factor was the use of fibers polished at a 45° angle. This improved the contact of fiber ends with adjacent tissue and, therefore, light collection. Another advantage of such optrodes is that they can be introduced into tissue without the aid of an insertion needle used previously. This resulted in a lower degree of tissue damage even when 325-μm fibers were used. The diameter of such an optrode varied between 325 and 975 μm along its length, which is comparable to the diameter of plunge needle electrodes used previously.[31]

Gains in signal quality allowed optical measurements even in blood-perfused hearts where optical signals are much weaker due to strong light absorption by hemoglobin. Perfusion with Tyrode's solution is known to cause a slow change of electrophysiological tissue properties during the course of experiment,[32] which is partially caused by tissue edema. Perfusion with blood significantly reduced tissue edema and thus provided for better preservation of tissue properties.

SN_{rms} decreased over time at the rate of approximately 33% per hour. This is consistent with the rate of signal decay measured using surface optical mapping[3] and reflects washout and photobleaching of the voltage-sensitive dye. Significantly faster signal deterioration was reported previously in optrode measurements.[24] A higher rate of signal decay in that study was probably caused by a much stronger intensity of excitation light and longer light exposures associated with averaging of multiple consecutive beats that resulted in faster dye photobleaching.

Comparison of Optical and Electrical Recordings

Electrical mapping with plunge needle electrodes was used previously to map intramural activation, repolarization and ARI as a substitute for APD measurements.[33,34] This assumes a close correspondence between electrical and optical measurements but direct experimental verification of this relationship is lacking. Furthermore, previous measurements utilizing optrodes and plunge electrodes reported significant differences between electrically and optically measured ATs as well as between APD and ARI.[35] Such differences were explained by a larger interrogation volume in electrical recordings in comparison to optical recordings. An alternative explanation could be the spatial separation between optical and electrical recording sites. Results obtained here are more consistent with the second explanation. Both ATs and APD measurements were very similar and highly correlated with changes of CL when

measured from closely adjacent sites. Such close correspondence justifies the use of ARI measurements as a substitute of APD.

Intramural APD heterogeneity

Spatial heterogeneities of repolarization and APD are considered important factors in arrhythmogenesis.[21,22] One of the major reasons for electrophysiological heterogeneity is the existence of "M cells" in the mid-myocardium that respond to slowing in pacing rate and inhibition of potassium currents by prolonging APD to a much greater extent than cells in epicardial and endocardial regions.[36] Until recently, intramural APD heterogeneities were most often measured using microelectrodes and surface optical mapping in isolated cells and in wedge preparations.[21,22,37] Optrodes offer a possibility to characterize electrophysiological heterogeneities in the intact hearts. Optrode measurements of intramural APD performed here did not reveal significant differences in APD values across the LV wall in porcine hearts. Slowing of pacing rate and blocking of potassium currents with d-sotalol or dofetilide, which were used previously to expose M cells,[26,27] did not increase intramural APD differences either. The lack of M cells is consistent with previous measurements in isolated tissue preparations of porcine LV myocardium.[30] As argued previously,[38] their absence may be related to the young age of animals (≈8–10 weeks) used in that and in the present studies.

Optrode measurements of shock-induced ΔV_m

Measurements of intramural V_m changes are critical for understanding the mechanism of defibrillation. Previously, intramural ΔV_m were measured only in wedge preparations using surface optical mapping.[16] Although these studies provided valuable information about shock effects, their extrapolation to whole hearts is limited by the differences in tissue properties and boundary conditions at the cut transmural surface of wedge preparations vs. the ones in the intact LV, which necessitates mapping of intramural ΔV_m in the intact hearts.

Optrode measurements of ΔV_m in porcine hearts performed in the present study revealed similarities as well as important differences from ΔV_m measurements in wedge preparations. Similarly to wedge preparations, shocks produced intramural ΔV_m. In contrast, the magnitude of these changes was significantly larger in the optrode recordings in comparison to wedge mapping. This can be attributed to a higher spatial resolution of optrode recordings and, therefore, to a smaller degree of spatial averaging in comparison to surface optical mapping. In wedge mapping experiments, strong shocks produced globally negative ΔV_m that didn't change sign upon changing the shock polarity, which was attributed to "virtual electrodes" formed at microscopic tissue discontinuities.[16] In contrast, positive polarizations were detected by optrodes even at the strongest shocks and the ΔV_m sign reversed with change in the shock polarity. Such differences in ΔV_m behavior may be due to the differences between wedge preparations and whole hearts. Alternatively, the discrepancies between the optrode and wedge mapping data could be due to the effect of optrodes on ΔV_m. It was shown in computer simulations that, with appropriate orientation of the shock field, plunge electrodes provide a substrate for shock-induced polarizations.[39] The optrodes may possibly cause the same effect. The role of optrodes in shock-induced ΔV_m requires further investigation.

Conclusions

The quality of optrode recordings was substantially improved, which should facilitate a development of 3-dimensional mapping. The optrodes can be used for high-fidelity intramural measurements of activation and repolarization times. Measurements of shock-induced V_m changes, however, may be affected by the optrode itself; this question requires further investigation.

Acknowledgements

This work was supported by NIH grants HL 67748 and HL28429. We would like to thank Dr. Alexey Zaitsev for his help in setting up a system for blood perfusion, and Reuben Collins and Frank Vance for their technical support.

This work was supported by NIH grants HL 67748 and HL28429

References

1. Rosenbaum, DS.; Jalife, J., editors. Optical Mapping of Cardiac Excitation and Arrhythmias. Armonk, NY: Futura; 2001.
2. Choi BR, Salama G. Simultaneous maps of optical action potentials and calcium transients in guinea-pig hearts: mechanisms underlying concordant alternans. J Physiol 2000;529:171–88. [PubMed: 11080260]
3. Fast VG, Ideker RE. Simultaneous optical mapping of transmembrane potential and intracellular calcium in myocyte cultures. J Cardiovasc Electrophysiol 2000;11:547–556. [PubMed: 10826934]
4. Laurita KR, Singal A. Mapping action potentials and calcium transients simultaneously from the intact heart. Am J Physiol 2001;280:H2053–2060.
5. Kong W, Walcott GP, Smith WM, Johnson PL, Knisley SB. Emission ratiometry for simultaneous calcium and action potential measurements with coloaded dyes in rabbit hearts: reduction of motion and drift. J Cardiovasc Electrophysiol 2003;14:76–82. [PubMed: 12625615]
6. Fast VG, Kléber AG. Microscopic conduction in cultured strands of neonatal rat heart cells measured with voltage-sensitive dyes. Circ Res 1993;73:914–925. [PubMed: 8403261]
7. Rohr S, Kucera JP, Fast VG, Kleber AG. Paradoxical improvement of impulse conduction in cardiac tissue by partial cellular uncoupling. Science 1997;275:841–844. [PubMed: 9012353]
8. Choi BR, Liu T, Salama G. The distribution of refractory periods influences the dynamics of ventricular fibrillation. Circ Res 2001;88:E49–58. [PubMed: 11249880]
9. Zaitsev AV, Guha PK, Sarmast F, Kolli A, Berenfeld O, Pertsov AM, de Groot JR, Coronel R, Jalife J. Wavebreak formation during ventricular fibrillation in the isolated, regionally ischemic pig heart. Circ Res 2003;92:546–553. [PubMed: 12600877]
10. Akar FG, Rosenbaum DS. Transmural electrophysiological heterogeneities underlying arrhythmogenesis in heart failure. Circ Res 2003;93:638–45. [PubMed: 12933704]
11. Omichi C, Lamp ST, Lin SF, Yang J, Baher A, Zhou S, Attin M, Lee MH, Karagueuzian HS, Kogan B, Qu Z, Garfinkel A, Chen PS, Weiss JN. Intracellular Ca dynamics in ventricular fibrillation. Am J Physiol 2004;286:H1836–H1844.
12. Katra RP, Laurita KR. Cellular mechanism of calcium-mediated triggered activity in the heart. Circ Res 2005;96:535–542. [PubMed: 15718502]
13. Weiss JN, Qu Z, Chen PS, Lin SF, Karagueuzian HS, Hayashi H, Garfinkel A, Karma A. The dynamics of cardiac fibrillation. Circulation 2005;112:1232–40. [PubMed: 16116073]
14. Lakkireddy V, Bub G, Baweja P, Syed A, Boutjdir M, El-Sherif N. The kinetics of spontaneous calcium oscillations and arrhythmogenesis in the in vivo heart during ischemia/reperfusion. Heart Rhythm 2006;3:58–66. [PubMed: 16399055]
15. Efimov IR, Cheng Y, Van Wagoner DR, Mazgalev T, Tchou PJ. Virtual electrode-induced phase singularity. A basic mechanism of defibrillation failure. Circ Res 1998;82:918–925. [PubMed: 9576111]
16. Fast VG, Sharifov OF, Cheek ER, Newton J, Ideker RE. Intramural virtual electrodes during defibrillation shocks in left ventricular wall assessed by optical mapping of membrane potential. Circulation 2002;106:1007–1014. [PubMed: 12186808]
17. Frazier DW, Krassowska W, Chen P-S, Wolf PD, Daniely ND, Smith WM, Ideker RE. Transmural activations and stimulus potentials in three-dimensional anisotropic canine myocardium. Circ Res 1988;63:135–146. [PubMed: 3383372]
18. El-Sherif N, Chinushi M, Caref EB, Restivo M. Electrophysiological mechanism of the characteristic electrocardiographic morphology of torsade de pointes tachyarrhythmias in the long-QT syndrome: detailed analysis of ventricular tridimensional activation patterns. Circulation 1997;96:4392–4399. [PubMed: 9416909]

19. Chattipakorn N, Fotuhi PC, Chattipakorn SC, Ideker RE. Three-dimensional mapping of earliest activation after near-threshold ventricular defibrillation shocks. J Cardiovasc Electrophysiol 2003;14:65–69. [PubMed: 12625612]
20. Pogwizd SM. Nonreentrant mechanisms underlying spontaneous ventricular arrhythmias in a model of nonischemic heart failure in rabbits. Circulation 1995;92:1034–1048. [PubMed: 7543829]
21. Yan GX, Shimizu W, Antzelevitch C. Characteristics and distribution of M cells in arterially perfused canine left ventricular wedge preparations. Circulation 1998;98:1921–1927. [PubMed: 9799214]
22. Akar FG, Yan GX, Antzelevitch C, Rosenbaum DS. Unique topographical distribution of M cells underlies reentrant mechanism of torsade de pointes in the long-QT syndrome. Circulation 2002;105:1247–1253. [PubMed: 11889021]
23. Trayanova N. Concepts of ventricular defibrillation. Phil Trans R Soc Lond A 2001;359:1327–1337.
24. Hooks DA, LeGrice IJ, Harvey JD, Smaill BH. Intramural multisite recording of transmembrane potential in the heart. Biophysical Journal 2001;81:2671–2680. [PubMed: 11606280]
25. Byars JL, Smith WM, Ideker RE, Fast VG. Development of optrode for transmural multisite optical recordings of Vm in the heart. J Cardiovasc Electrophysiol 2003;14:1196–1202. [PubMed: 14678134]
26. Sicouri S, Moro S, Elizari MV. d-Sotalol Induces Marked Action Potential Prolongation and Early Afterdepolarizations in M but Not Empirical or Endocardial Cells of the Canine Ventricle. J Cardiovasc Pharmacol Ther 1997;2:27–38. [PubMed: 10684439]
27. Obreztchikova MN, Sosunov EA, Plotnikov A, Anyukhovsky EP, Gainullin RZ, Danilo P, Yeom ZH, Robinson RB, Rosen MR. Developmental changes in IKr and IKs contribute to age-related expression of dofetilide effects on repolarization and proarrhythmia. Cardiovasc Res 2003;59:339–50. [PubMed: 12909317]
28. Haws CW, Lux RL. Correlation between in vivo transmembrane action potential durations and activation-recovery intervals from electrograms. Effects of interventions that alter repolarization time. Circulation 1990;81:281–8. [PubMed: 2297832]
29. Holley LK, Knisley SB. Transmembrane potentials during high voltage shocks in ischemic cardiac tissue. PACE 1997;20:146–152. [PubMed: 9121979]
30. Rodriguez-Sinovas A, Cinca J, Tapias A, Armadans L, Tresanchez M, Soler-Soler J. Lack of evidence of M-cells in porcine left ventricular myocardium. Cardiovasc Res 1997;33:307–13. [PubMed: 9074694]
31. Kovoor P, Campbell C, Wallace E, Byth K, Dewsnap B, Eipper V, Uther J, Ross D. Effects of simultaneous insertion of 66 plunge needle electrodes on myocardial activation, function, and structure. PACE 2003;26:1979–85. [PubMed: 14516338]
32. Arbel ER, Prabhu R, Ramesh V, Pick R, Glick G. A perfused canine right bundle branch-septal model for electrophysiological studies. Am J Physiol 1979;236:H379–84. [PubMed: 420322]
33. Newton JC, Smith WM, Ideker RE. Estimated global transmural distribution of activation rate and conduction block during porcine and canine ventricular fibrillation. Circ Res 2004;94:836–42. [PubMed: 14764451]
34. Zhang YZ, He B, Wang LX. Effect of an increase in coronary perfusion on transmural ventricular repolarization. Physiol Res. 2006
35. Caldwell BJ, Legrice IJ, Hooks DA, Tai DC, Pullan AJ, Smaill BH. Intramural measurement of transmembrane potential in the isolated pig heart: validation of a novel technique. J Cardiovasc Electrophysiol 2005;16:1001–10. [PubMed: 16174023]
36. Antzelevitch C, Shimizu W, Yan GX, Sicouri S, Weissenburger J, Nesterenko VV, Burashnikov A, Di Diego J, Saffitz J, Thomas GP. The M cell: its contribution to the ECG and to normal and abnormal electrical function of the heart. J Cardiovasc Electrophysiol 1999;10:1124–1152. [PubMed: 10466495]
37. Sicouri S, Fish J, Antzelevitch C. Distribution of M cells in the canine ventricle. J Cardiovasc Electrophysiol 1994;5:824–37. [PubMed: 7874328]
38. Antzelevitch C. Are M cells present in the ventricular myocardium of the pig? A question of maturity. Cardiovasc Res 1997;36:127–8. [PubMed: 9415281]
39. Langrill DM, Roth BJ. The effect of plunge electrodes during electrical stimulation of cardiac tissue. IEEE Trans Biomed Eng 2001;48:1207–1211. [PubMed: 11585046]

Lists of Abbreviations

V_m
membrane potential

APA
action potential amplitude

APD
action potential duration

APD_{80}
action potential duration at the 80% level of repolarization

AT
activation time

AT_e
electrical activation time

AT_o
optical activation time

CL
cycle length

LED
light-emitting diode

PDA
photodiode array

SN_{rms}
signal-to-noise ratio

Sub-Endo
sub-endocardium

Mid
mid-myocardium

Sub-Epi
sub-epicardium

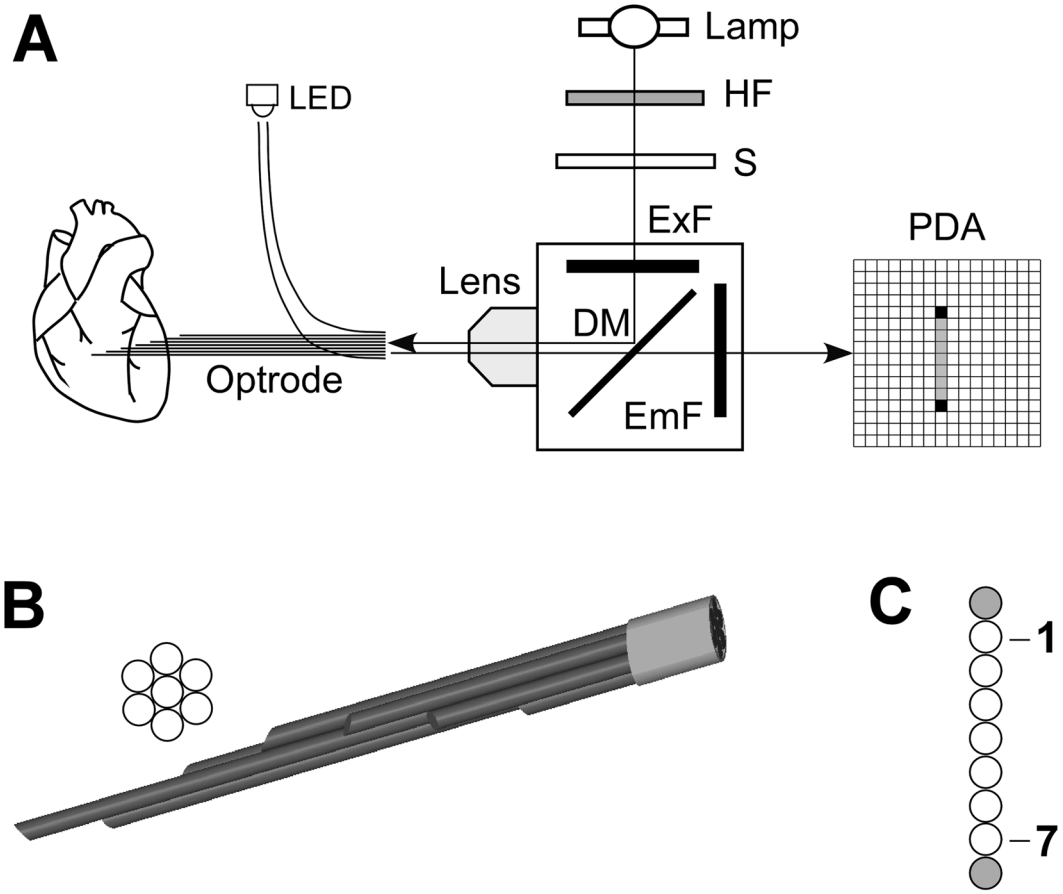

Figure 1.

Panel A, Schematic diagram of the optical system. HF, heat filter; S, electromechanical shutter; ExF, excitation filter; DM, dichroic mirror; PDA, 16×16 photodiode array. Panel B, View of the cross section of an optrode and its tissue end. Fibers are arranged hexagonally with ends spaced at 2 or 3 mm intervals. Panel C, View of the optrode detector end. Blank circles in the middle represented seven measurement fibers; two shaded circles depict fibers used for alignment. This linear fiber array is projected onto a column of nine photodiodes in the PDA.

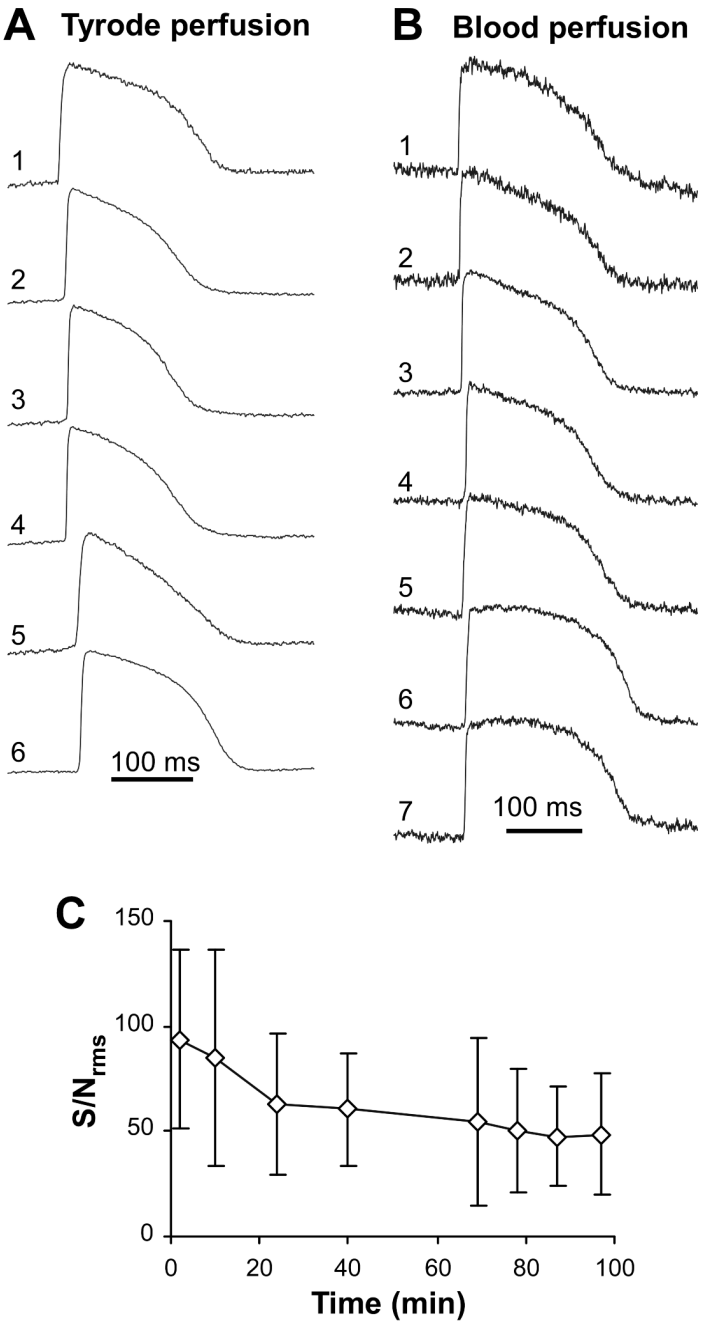

Figure 2.

Optrode recordings of intramural action potentials. Panel A, Intramural action potentials measured with a 325-μm fiber optrode in a porcine heart perfused with Tyrode solution. Numbers 1 through 6 designate recordings obtained from sub-epicardium through sub-endocardium. One fiber was outside the muscle in the cavity (not shown). Panel B, Intramural action potentials measured in a blood perfused heart. Panel C, Reduction of the average signal-to-noise ratio (SN_{rms}) during the time of experiment in one heart.

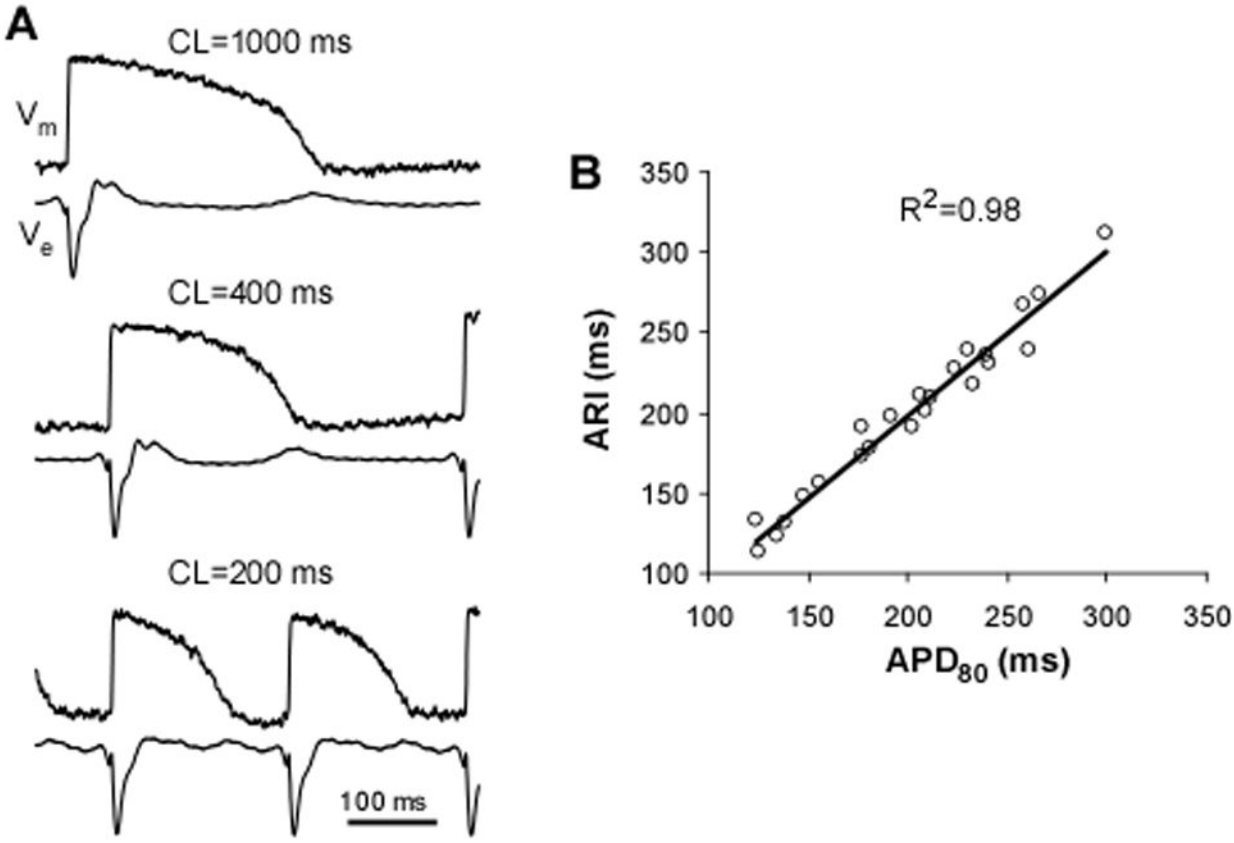

Figure 3.

Comparison of optical and electrical recordings. Panel A, Simultaneous recordings of optical action potential (V_m) and extracellular electrical potential (V_e) at different cycle length (CL). The optical recordings were made using a 225-μm fiber; electrical signals were made using a closely adjacent plunge needle electrode. Panel B, Correlation between APD_{80} and ARI with variation of CL between 200 and 1000 ms. Straight line depicts linear regression.

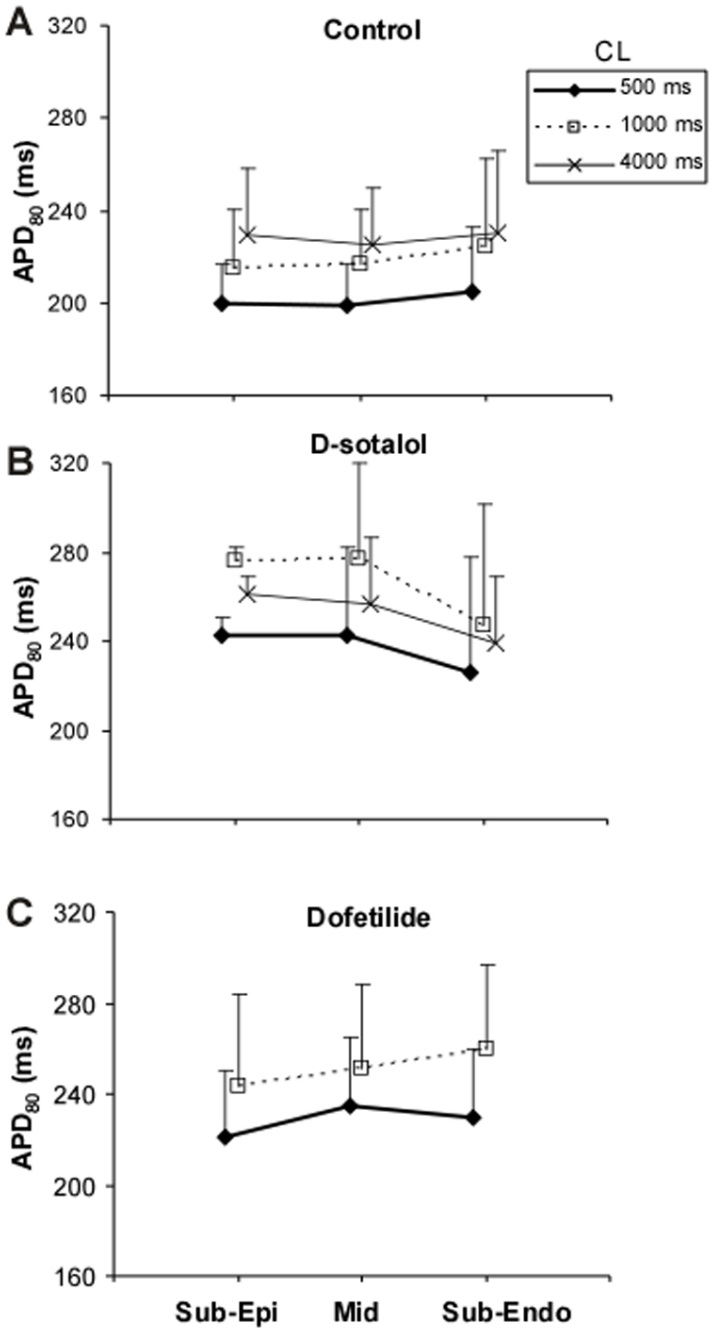

Figure 4.

Intramural APD distribution. Panel A, APD_{80} measured in sub-epicardial (Sub-Epi), mid-myocardial (Mid) and sub-endocardial (Sub-Endo) muscle layers at pacing CL of 0.5, 1 and 4 s in control conditions. The data were obtained from 5 hearts perfused with either Tyrode solution or blood. Panels B and C, APD_{80} in different tissue layers in the presence of 125 μM of d-sotalol (B) and 2 μM of dofetilide (C).

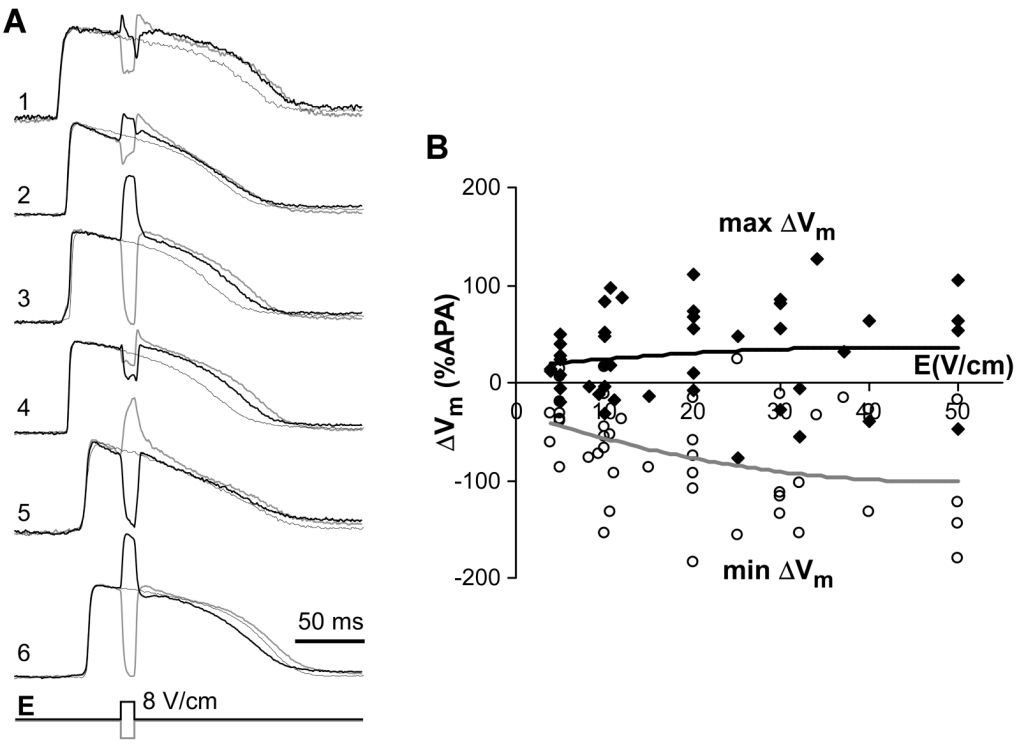

Figure 5.

Optical measurements of shock-induced ΔV_m. Panel A, Intramural V_m recordings in control and during application of 8-V/cm shocks of two polarities. Recording 1 was obtained form sub-epicardium, recording 6 from sub-endocardium. Panel B, Dependences of minimal and maximal ΔV_m magnitude on the shock strength. Solid lines depict second-order polynomial fits of the data.